Polynomial curve fitting method for refraction-angle extraction in diffraction enhanced imaging[*]

CHEN Zhi-Qiang(陈志强)[1,2]　　DING Fei(丁飞)[1,2]　　HUANG Zhi-Feng(黄志峰)[1,2;1)]　　ZHANG Li(张丽)[1,2]

YIN Hong-Xia(尹红霞)[3]　　WANG Zhen-Chang(王振常)[3]　　ZHU Pei-Ping(朱佩平)[4]

1 (Department of Engineering Physics, Tsinghua University, Beijing 100084, China)
2 (Key Laboratory of Particle & Radiation Imaging (Tsinghua University), Ministry of Education Beijing 100084, China)
3 (Medical Imaging Center, Beijing Tongren Hospital, Capital Medical University, Beijing 100730, China)
4 (Beijing Synchrotron Radiation Facility, Institute of High Energy Physics,
Chinese Academy of Sciences, Beijing 100049, China)

Abstract　X-ray diffraction enhanced imaging (DEI) is applied to inspect internal structures of weakly absorbing low-Z sample. How to extract phase information from raw images measured in different positions of rocking curve is the key problem of DEI. In this paper, we present an effective extraction method called polynomial curve fitting method, in order to extract accurate information angular in a fast speed. It is compared with the existing methods such as multiple-images statistical method and Gaussian curve fitting method. The experiments results on a plastic cylinder and a black ant at the Beijing Synchrotron Radiation Facility prove that the polynomial curve fitting method can obtain most approximate refraction-angle values and its computation speed is 10 times faster than the Gaussian curve fitting method.

Key words　diffraction enhanced imaging, synchrotron radiation, polynomial curve fitting

PACS　42.30.Rx, 42.30.Va, 41.60.Ap

1　Introduction

Diffraction enhanced imaging (DEI) based on synchrotron radiation is a non-destructive testing and diagnostic technology. Phase contrast imaging using perfect crystals was presented by Davis et al.[1], and the conception of the DEI was first developed by Chapman et al at the National Synchrotron Light Source (NSLS) in 1996[2, 3]. Using the high angular resolution of perfect crystals, DEI provides extremely high sensitivity and contrast of weakly absorbing low-Z objects which have many elaborate details such as breast cancers[4]. In recent years, researchers have also made a breakthrough on the extraction and computed tomography methods of the DEI system to access good results[5—7]. Therefore, DEI has become a helpful inspection method in the medical and biological fields[8].

In general for X-rays, the complex refractive in-

dex of a sample can be expressed as $n = 1 - \delta - i\beta$, where δ determines the phase shift (ϕ) of the X-ray when passing through the sample, while β is correlated with the linear absorption coefficient μ. δ is also named refractive index decrement[9]. Actually, δ is mostly a thousand times larger than β[10]. DEI calculates differential phase shifts ($\Delta\phi$) by measuring the refraction-angle values of refracted X-rays. Chapman et al developed a geometric optics approximation (GOA) method to extract the refraction-angle images from two DEI images[2]. But the Taylor approximation in GOA method limits the applicability and induces unwanted error. In order to improve this problem, a nonlinear extension method (EDEI) was provided by AntoMaksimenko in 2007[11]. And it improves the accuracy of the results and makes the sensitivity limit wider under the same experiment condition as the GOA method. At the same time, Rigon L presents a three-image DEI algorithm (GDEI) to decouple the information of absorption, re-

fraction, and ultrasmall-angle scattering. It is worth noting that three DEI images in this method can be collected at any differential position of the Rocking Curve (RC).[12, 13] According to the symmetry characteristics of RC, the alternative extraction method with the images collected at one-side of RC has been developed[14].

But the resultant images calculated by these methods have low signal noise ratio (SNR) in experiment. Then, several methods using multiple DEI images based on statistical analysis were developed by Oltulu[15], Wemick[16] and Pagot[17] et al. Their formulae of the extracting refraction-angle images from multiple DEI images are all based on statistical theory. Their methods are grouped together and named 'multiple-images statistical (MIS)' method here. Huang et al investigated the limitations of GOA and MIS methods, then presented three more accurate extraction methods: the statistical geometric optics approximation (S-GOA) method, the maximum refraction-angle (MRA) method and the Gaussian curve fitting (GCF) method[18—21]. The GCF method provides the most approximate refraction-angle values, but it has high degree of computation complexity due to the nonlinear multiplex iterative process. So the enormous calculation time obviously limits the practical application of the GCF method.

In this paper, we present a polynomial curve fitting (PCF) method to speed up the computation time. This paper is constructed as follows: The principle of DEI system at the Beijing Synchrotron Radiation Facility (BSRF) is introduced in Section 2. The existing extraction methods based on multiple images are briefly reviewed in Section 3. In Section 4, the principle of PCF method is presented detailedly. Based on the experimental results at the BSRF, comparisons of PCF and the existing methods are described in Section 5. Finally, the conclusion on PCF method is drawn in Section 6.

2   Principle of DEI system

The schematic diagram of the DEI setup at the BSRF is shown in Fig. 1. A white beam from the synchrotron radiation source is monochromatized by the monochromator. Then the monochromatic X-ray beam passes through a weakly absorbing low-Z sample. The transmitted beam will change its direction of propagation slightly because of the refractive index's gradients of the sample. That is, the X-rays will be refracted a very small angle (arc-second) by the sample. The angle of propagation relative to the

initial propagation direction is

$$\Delta\theta \approx \frac{1}{k}\frac{\partial \Phi(x)}{\partial x} \tag{1}$$

where $\Phi(x)$ denotes the phase change in the x-direction and k is the wave number[1]. The refracted beam is diffracted by the analyzer before the CCD camera. If the incident angle of the beam is equal to the Bragg angle, the beam is diffracted furthest by the analyzer according to the Bragg diffraction theory. The full-width at half-maximum (FWHM) of the RC is usually regarded as Darwin width of the crystal in experiment.
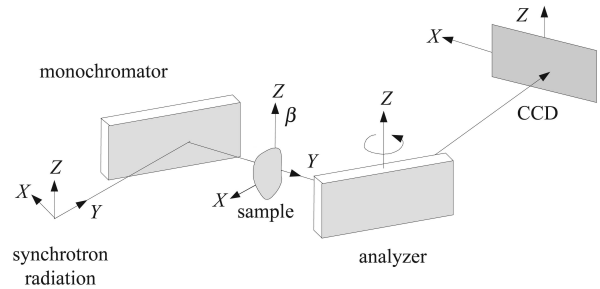

Fig. 1.   The schematic diagram of the DEI experimental system at the BSRF.

3   Existing methods using multiple images

According to the theory of X-ray diffraction by perfect crystals, if the analyzer is set in the position of the peak of the RC, the refractive beam has maximum intensity, so the center of the RC is close to the actual refraction-angle value. The refraction-angle can be calculated by the following process: Two groups (a sample group and a background group) of the DEI images are measured in dozens of positions of the RC. Suppose there are M positions totally. For each position θ_n, $I_s(n)$ denotes the intensity of the DEI image with the sample and $I_{bg}(n)$ denotes the intensity of the DEI image without the sample. $R_s(\theta)$ denotes the sample RC and $R_{bg}(\theta)$ denotes the background RC.

There are two existing extraction methods as follows:

1) Multiply-image statistical (MIS) method

In theory, the centre value of the sample (or background) RC is equal to the centroid value of the sample (or background) RC if the sample (or background) RC is sampled continuously and infinitely. The MIS method regards the centroid as the center of the RC[15], so the refraction-angle image can be

calculated by Formula (1):

$$\theta_{\mathrm{s}} = \sum_{n=1}^{M} \theta_n I_{\mathrm{s}}(n) \Big/ \sum_{n=1}^{M} I_{\mathrm{s}}(n),$$

$$\theta_{\mathrm{bg}} = \sum_{n=1}^{M} \theta_n I_{\mathrm{bg}}(n) \Big/ \sum_{n=1}^{M} I_{\mathrm{bg}}(n), \qquad (2)$$

$$(\Delta\theta)_{\mathrm{MIS}} = \theta_{\mathrm{s}} - \theta_{\mathrm{bg}}.$$

However, the sampling range and the measured positions are limited in experiment. So the refraction-angle values extracted by the MIS method are always smaller than the actual values. This is the limitation of the MIS method[20].

2) Gaussian curve fitting (GCF) method

The GCF method applies GCF algorithm to fit the sample (or background) RC to obtain the center value. Thus, the refraction-angle image can be calculated by Formula (3):

$$(\Delta\theta)_{\mathrm{GCF}} = \theta_{\mathrm{peak,sm}} - \theta_{\mathrm{peak,bg}} \qquad (3)$$

where $\theta_{\mathrm{peak,bg}}$, $\theta_{\mathrm{peak,sm}}$ denote the centers of the sample and background RCs, respectively. This approach presents the most approximate refraction-angle values and the highest SNR image from a series of DEI images[19, 21]. But the GCF method adopts the least-square method which is required to solve a set of complicated nonlinear equations. Therefore, the high computational complexity obviously limits the practical application of the GCF method.

4 Polynomial curve fitting (PCF) method

In theory，the sample (or background) RC can be described by the N-order polynomial approximately. The order N can be determined by the morphology of rocking curve. For example, our measured rocking curve is similar to the morphology of Sine-like function in a single period. Then, it can be fitted well by five-order polynomial approximately.

The expressions of the sample and the background RCs are defined in Formula (4).

$$R_{\mathrm{s}}(\theta_n) \approx F_{\mathrm{s}}(\theta_n, N) = \sum_{i=0}^{N} A_i \theta_n^i,$$

$$R_{\mathrm{bg}}(\theta_n) \approx F_{\mathrm{b}}(\theta_n, N) = \sum_{i=0}^{N} B_i \theta_n^i, \qquad (4)$$

where A_i, B_i denote the ith coefficient of N-orders polynomials $F_{\mathrm{s}}(\theta_n, N)$ and $F_{\mathrm{b}}(\theta_n, N)$, respectively. Using the least-square criterion shown in Formula (5), the coefficients (A_i, B_i) can be calculated by solving

the regular linear equation group, respectively, which is shown in Formula (6).

$$\sum_{i=0}^{M} [F_{\mathrm{s,b}}(\theta_i, N) - I_{\mathrm{s,b}}(\theta_i)]^2 = \min \qquad (5)$$

$$\begin{bmatrix} M+1 & \sum_{i=0}^{M}\theta_i & \cdots & \sum_{i=0}^{M}\theta_i^N \\ \sum_{i=0}^{M}\theta_i & \sum_{i=0}^{M}\theta_i^2 & \cdots & \sum_{i=0}^{M}\theta_i^{N+1} \\ \vdots & \vdots & \vdots & \vdots \\ \sum_{i=0}^{M}\theta_i^N & \sum_{i=0}^{M}\theta_i^{N+1} & \cdots & \sum_{i=0}^{M}\theta_i^{2N} \end{bmatrix} \begin{bmatrix} A_0, B_0 \\ A_1, B_1 \\ \vdots \\ A_N, B_N \end{bmatrix} =$$

$$\begin{bmatrix} \sum_{i=0}^{M} I_{\mathrm{s,b}}(\theta_i) \\ \sum_{i=0}^{M} \theta_i I_{\mathrm{s,b}}(\theta_i) \\ \vdots \\ \sum_{i=0}^{M} \theta_i^N I_{\mathrm{s,b}}(\theta_i) \end{bmatrix}. \qquad (6)$$

Actually, the center of the RC can be regarded as the position of the extreme point of polynomial curve. $\theta_{\mathrm{s,max}}$, $\theta_{\mathrm{b,max}}$ denote the positions of the extreme points of the sample and background RCs, respectively. The refraction-angle image can be calculated by Formula (7):

$$(\Delta\theta)_{\mathrm{GCF}} = \theta_{\mathrm{s,max}} - \theta_{\mathrm{b,max}}. \qquad (7)$$

The PCF method adopts the least-square method to solve a set of linear equations shown in Formula (6), so that the computational complexity of the PCF method is much lower than that of the GCF method. Thus, the PCF method costs less computation time.

5 Experiments

At the 4W1A Beamline of the BSRF, the tunable energy range of this system was 4—30 keV and the size of the X-ray beam was 20 mm × 10 mm. The analyzer's tunable precision was 0.05 arc-seconds. The CCD camera (Photonic Science X-ray FDI 18 mm) was read out at 1300×1030 matrix size, with 10.9 μm per pixel. The experimental data were processed by a Matlab 7.5 program with 2.00 GHz Xeon(R) CPU, 1.0 G bytes memory.

In order to compare the extraction capability of the refraction-angles using the above three methods, the difference ($[\Delta\theta]_{\text{Difference}}$) between the maximum and the minimum refraction-angle values is defined here:

$$[\Delta\theta]_{\text{Difference}} = [\Delta\theta]_{\max} - [\Delta\theta]_{\min} \qquad (8)$$

where $[\Delta\theta]_{\max}$, $[\Delta\theta]_{\min}$ denote the maximum and minimum refraction-angle values.
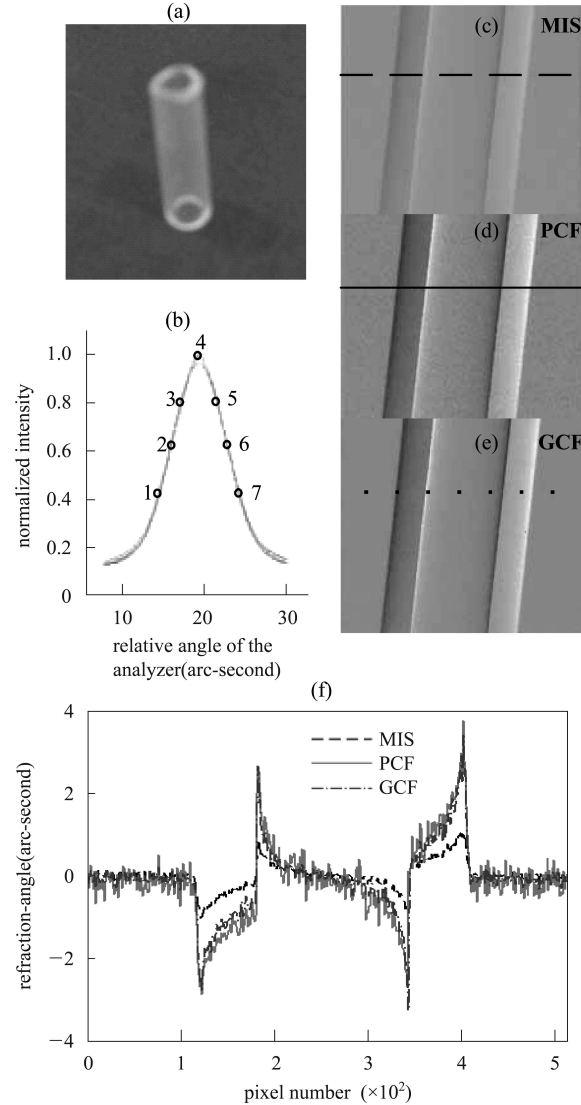

Fig. 2. The experimental results of the plastic cylinder. (a) The photograph; (b) 7 positions along the RC; (c)—(e) The refraction-angle images extracted by MIS, PCF and GCF methods, respectively; (f) The refraction-angle values along the marked lines are plotted together for comparison.

A plastic cylinder cut from a common ball-point pen was inspected in this experiment, as shown in Fig. 2(a). Its outside diameter was 3 mm and its inner diameter was 1.5 mm. 7 DEI images were measured

in different positions of the RC shown in Fig. 2(b). Three refraction-angle images extracted by different extraction methods are shown in Fig. 2(c)—(e) in the same gray window. The refraction-angle values of these methods along the marked line are plotted in Fig. 2(f). Finally, the computation time and the differences are listed in Table 1.

Table 1. The computation time and the differences of these methods.

method	MIS	GCF	PCF
time/s	27.6	15488	1447.3
difference (arc-second)	2.113	6.6543	6.6442

In Fig. 2, the refraction-angle image extracted by the MIS method has the smoothest noise but its refraction-angle absolute values are the smallest. The refraction-angle image extracted by the GCF method has the largest refraction-angle absolute values and the highest SNR, but its computation time is over 4 hours. The PCF method can extract as the same large refraction-angle absolute values as the GCF method, but its refraction-angle image has much noise because the polynomial fitting error is a little big based on 7 raw images. However, $[\Delta\theta]_{\text{Difference}}$ of the PCF method is much larger than that of the MIS method but it is only about 0.01 arc-seconds lower than that of the GCF method. Furthermore, the computation time of the PCF method is 10 times shorter than that of the GCF method.

Table 2. The computation time and the differences of three methods in the black ant experiment.

method	MIS	GCF	PCF
time/s	57.3	18388.7	1747.2
difference (arc-second)	1.5069	2.6153	2.6041

A small black ant with more complex structures was also inspected. 33 DEI images were measured in different positions of the RC in experiment. The refraction-angle images, the computation time and the differences ($[\Delta\theta]_{\text{Difference}}$) of the MIS, GCF and PCF methods are shown in Table 2, respectively. In Fig. 3, the refraction-angle image extracted by the MIS method has the smallest absolute values, while the PCF method has almost the same refraction-angle image as the GCF method. It's proved that 33 DEI images are enough for the PCF method to smooth the fitting noise. Note that the computation speed of the PCF method is also 10 times faster than that of the GCF method in this case.
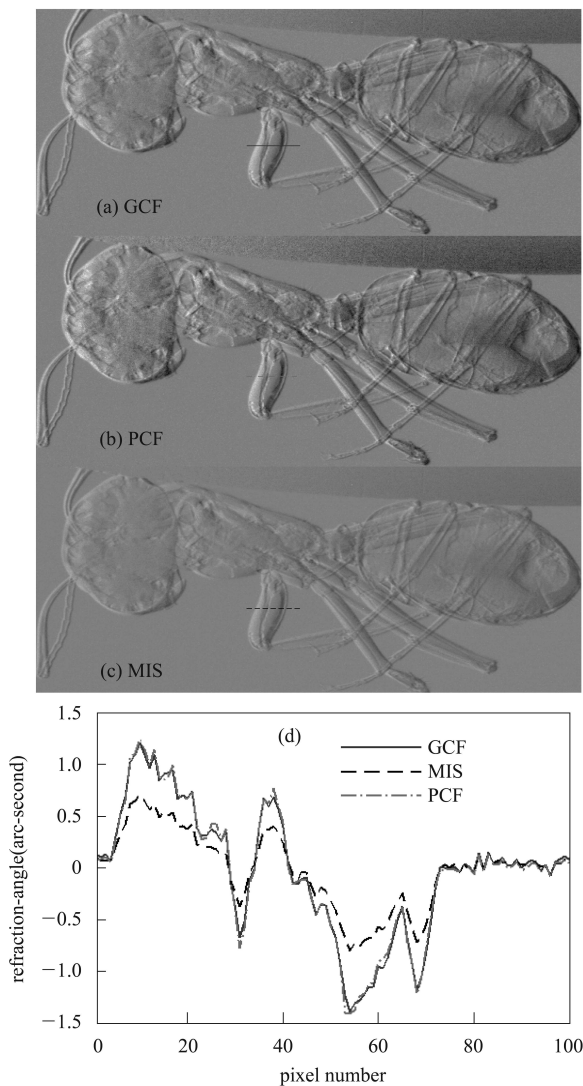
Fig. 3.   The experimental results of the black
ant. (a)—(c) The refraction-angle images ex-
tracted by the MIS, PCF and GCF methods,
respectively; (d) The refraction-angle values
along the marked lines are plotted together
for comparison.

Therefore, the PCF method can be taken instead
of the MIS and GCF methods in actual DEI exper-
iments to obtain most approximate refraction-angle
values within acceptable computation time. For ex-
ample, Fig. 4 shows that two refraction-angle im-
ages of a piece of human lung tissue are extracted
by the PCF and MIS method using 19 DEI images
along the RC. Obviously, the PCF method provides

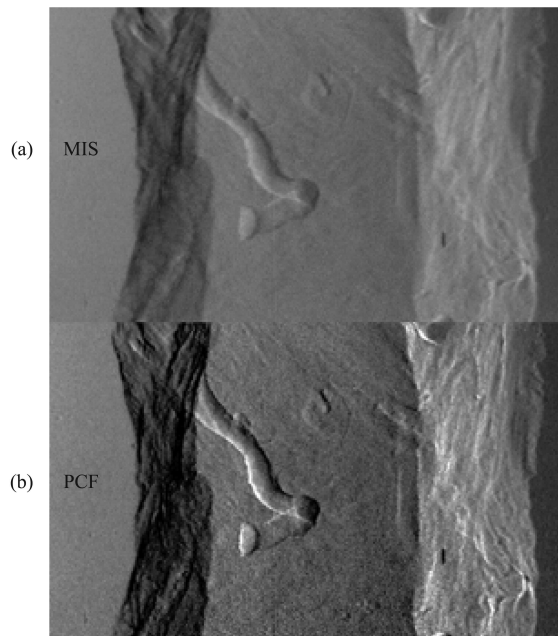much higher contrast of refraction-angle image than
the MIS method.

Fig. 4.   The experimental results of a piece of
human lung tissue. (a) The refraction-angle
image extracted by the MIS method; (b) The
refraction-angle image extracted by the PCF
method.

6   Conclusion

This paper presents a theoretical and experimen-
tal study on the polynomial curve fitting method
for refraction-angle extraction in DEI. The experi-
ments on the plastic cylinder with simple structures
and the black ant with complex structures prove
that the PCF method can obtain most approximate
refraction-angle values and its computation speed
is 10 times faster than the GCF method. But the
polynomial fitting error is a little bigger if the PCF
method adopts small amount of DEI images measured
along the RC. How to determinate the polynomial or-
der and reduce the errors will be further studied in
the future.

References

1 Davis T J, GAO D, Gureyev T E et al. Nature, 1995, **373**: 595—598
2 Chapman D, Thomlinson W, Arfelli F et al. Rev. Sci. Instrum., 1996, **67**: 3360 (published on CD-ROM)
3 Chapman D, Thomlinson W, Johnston R E et al. Phys. Med. Biol., 1997, **42**: 2015—2025
4 Chapman D, Pisano E, Thomlinson W et al. Breast Disease, 1998, **10**: 197—207
5 LIU Yi-Jin, ZHU Pei-Ping, CHEN Bo et al. Phys. Med. Biol., 2007, **52**: L5—L13
6 LIU Yi-Jin, ZHU Pei-Ping, CHEN Bo et al, Nucl. Instrum. Methods A, 2007, **580**: 617—620
7 ZHU Pei-Ping, YUAN Qing-Xi, HUANG Wan-Xia et al. J. Phys. D: Appl. Phys., 2006, **39**: 4142—4147
8 Bravin A. J. Phys. D: Appl. Phys., 2003, **36**: A24—A29
9 Michette A G, Buckley C J. X-ray Science and Technology, London, Institute of Physics publishing, 1993. 10—12
10 Momose A, Takeda T, Yoneyama A et al. Analytical Sciences, 2001, **17**: 527—530
11 Maksimenko A, Appl. Phys. Lett., 2007, **90**: 154106
12 Rigon L, Arflli F, Menk. Appl. Phys. Lett., 2007, **90**: 114102
13 Rigon L, Arflli F, Menk, J. Phys. D: Appl. Phys., 2007, **40**: 3077—3089
14 Hasnah M O, Chapman D. Nuclear Instrument and Methods in Physics Research A, 2008, **584**: 424—427
15 Oltulu O, ZHONG Z, Hasnah M et al. J. Phys. D: Appl. Phys., 2003, **36**: 2152—2155
16 Wernick M N, Wirjadi O, Chapman D et al. Phys. Med. Biol., 2003, **48**: 3875—3895
17 Pagot E, Cloetens P, Fiedler S et al. Appl. Phys. Lett., 2003, **82**: 3421—3423
18 HUANG Zhi-Feng, LI Zheng, KANG Ke-Jun et al. HEP & NP, 2005, **29**:(supp.): 133—136 (in Chinese)
19 HUANG Zhi-Feng, KANG Ke-Jun, YANG Yi-Gang. Nuclear Instruments and Methods in Physics Research A, 2007, **579**: 218—222
20 HUANG Zhi-Feng, KANG Ke-Jun, LI Zheng. Physics in Medicine and Biology, 2006, **51**: 3031—3039
21 HUANG Zhi-Feng, KANG Ke-Jun, ZHU Pei-Ping et al. Physics in Medicine and Biology, 2007 **52**: 1—12